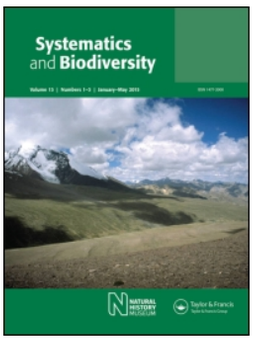

Systematics and Biodiversity

ISSN: 1477-2000 (Print) 1478-0933 (Online) Journal homepage: http://www.tandfonline.com/loi/tsab20

Morphology and phylogeny of two new ciliates, Sterkiella sinica sp. nov. and Rubrioxytricha tsinlingensis sp. nov. (Protozoa, Ciliophora, Hypotrichia) from north-west China

Lingyun Chen, Xiaolu Zhao, Chen Shao, Miao Miao & John C. Clamp

To cite this article: Lingyun Chen, Xiaolu Zhao, Chen Shao, Miao Miao & John C. Clamp (2017) Morphology and phylogeny of two new ciliates, Sterkiella sinica sp. nov. and Rubrioxytricha tsinlingensis sp. nov. (Protozoa, Ciliophora, Hypotrichia) from north-west China, Systematics and Biodiversity, 15:2, 131-142, DOI: 10.1080/14772000.2016.1219426

To link to this article: http://dx.doi.org/10.1080/14772000.2016.1219426

Published online: 06 Oct 2016.

Systematics and Biodiversity (2017), **15(2)**: 131–142

Taylor & Francis
Taylor & Francis Group

Research Article

Morphology and phylogeny of two new ciliates, *Sterkiella sinica* sp. nov. and *Rubrioxytricha tsinlingensis* sp. nov. (Protozoa, Ciliophora, Hypotrichia) from north-west China

LINGYUN CHEN[1,2], XIAOLU ZHAO[2], CHEN SHAO[1], MIAO MIAO[3] & JOHN C. CLAMP[4]

[1]The Key Laboratory of Biomedical Information Engineering, Ministry of Education, School of Life Science and Technology, Xi'an Jiaotong University, Xi'an 710049, China
[2]Institute of Evolution & Marine Biodiversity, Ocean University of China, Qingdao 266003, China
[3]Savaid Medical School, University of Chinese Academy of Sciences, Beijing 100049, China
[4]Department of Biology, North Carolina Central University, Durham, 1801 Fayetteville St., North Carolina 27707, USA

(Received 4 May 2016; accepted 19 July 2016; published online 6 October 2016)

Two new hypotrichous ciliates, *Sterkiella sinica* sp. nov. and *Rubrioxytricha tsinlingensis* sp. nov., were isolated from two different locations in China (the former from the upper 10 cm of soil in the Sangke Grassland, southern Gansu Province and the latter from a freshwater pond in the northern part of the Tsinling Mountains, south-western Shaanxi Province). We describe their morphology, infraciliature, and molecular phylogeny. Compared with its congeners, *S. sinica* sp. nov. is characterized by an elongate oval to elliptical shape with the anterior end narrowly rounded and the posterior end broadly rounded, consistently 18 frontoventral transverse cirri, cirrus III/2 farther toward the anterior than cirrus IV/3 and closer to cirrus IV/3 than to paroral, cirrus V/3 closer to cirrus V/4 than cirrus V/2, cirrus V/2 closer to cirrus VI/2 than cirrus V/3, three caudal cirri narrowly separated and not elongated, and terrestrial habitat. Compared with its congeners, *R. tsinlingensis* sp. nov. is characterized by a length *in vivo* of 100–180 μm, yellow-brown in colour, two macronuclear nodules and two or three micronuclei, yellow-green cortical granules, marginal rows almost confluent posteriorly, six dorsal kineties and three caudal cirri, caudal cirri and dorsal bristles almost indistinguishable when viewed *in vivo*, and freshwater habitat. Phylogenetic analyses based on small-subunit rRNA sequences revealed *S. sinica* sp. nov. associates most closely with *Sterkiella* sp. JS-2012d although the genus *Sterkiella* is not monophyletic. *Rubrioxytricha tsinlingensis* sp. nov. and *R. ferruginea* cluster together within a clade that also includes *R. haematoplasma*, *Ponturostyla enigmatica* and *Pseudocyrtohymena koreana*.

http://www.zoobank.org/urn:lsid:zoobank.org:pub:27060A1C-F0D4-4FB2-866A-66F939B12105

Key words: Hypotrichia, infraciliature, new species, phylogeny, *Rubrioxytricha*, *Sterkiella*, taxonomy

Introduction

Ciliates in the subclass Hypotrichia Stein, 1859, have been a consistent focus of ciliatological research and now number over 1000 nominal species that exhibit extremely diverse morphological and morphogenetic features (e.g. Berger, 1999, 2006, 2008, 2011; Bharti, Kumar, & Terza, 2015; Bourland, 2015; Fan et al., 2015; Hu & Kusuoka, 2015; Kahl, 1932; Li, Chen, & Xu, 2016; Luo et al., 2015; Paiva, Shao, Fernandes, Borges, & Silva-Neto, 2016; Pan et al., 2016; Shao, Chen, Pan, Warren, & Miao, 2014; Song, Warren, & Hu, 2009). Recently, morphogenetic data have been used to discriminate between morphologically similar hypotrich ciliates (Chen, Huang, & Song, 2011; Fan, Lu, Huang, Hu, & Warren, 2016; Kim, Vďačný, Shazib, & Shin, 2014; Kumar & Foissner, 2015; Kumar et al., 2015; Singh & Kamra, 2015a). Moreover, some recent phylogenetic analyses have led to a better understanding of systematics and evolutionary relationships (Gao et al., 2016; Gao, Yi, Gong, Al-Rasheid, & Song, 2010; Huang, Yi, Al-Farraj, & Song, 2010; Lv, Shao, Yi, & Warren, 2015; Wang, Gao, Huang, Strüeder-Kypke, & Yi, 2015; Yi & Song, 2011; Yi, Dunthorn, Song, & Stoeck, 2010; Yi, Lin, Warren, Al-Rasheid, & Song, 2010; Zhao, Gao, Fan, Strüeder-Kypke, & Huang, 2015).

Correspondence to: C. Shao. Email: andrews1201@hotmail.com and M. Miao. Email: doublemiao@126.com

ISSN 1477-2000 print / 1478-0933 online

http://dx.doi.org/10.1080/14772000.2016.1219426

The genus *Sterkiella* was established by Foissner, Blatterer, Berger and Kohmann (1991) which is characterized by its rigid or only slightly flexible body; curved and intersecting undulating membranes; marginal rows separated and the presence of caudal cirri (Berger, 1999). The genus *Rubrioxytricha* was established by Berger (1999) for two former species of *Oxytricha* that possess one or two caudal cirri and homogeneously coloured cytoplasm (Berger, 1999).

In July 2011 and April 2013, two oxytrichid ciliates new to science, one of which could be assigned to *Sterkiella* and the other to *Rubrioxytricha*, were isolated from localities in north-western China. In the present paper, we provide detailed descriptions of the morphology of each species and phylogenetic analyses based on sequences of small subunit (SSU) rRNA that confirm the validity of the new species.

Materials and methods

Sampling, culturing, and isolation

Sterkiella sinica sp. nov. was isolated from the surface layer of soil in the Sangke Grassland (35 °06′N, 102 °25′E), Gansu Province when the air temperature was 14 °C and the pH measured 8.6 using a pH meter. Five samples (*c*. 500 g each) were taken in July 2011, air-dried for one month, sealed in a large paper envelope for ventilation, and investigated during June to December 2012. Most of the Sangke Grassland is over 3000 m above sea level. Its mean annual temperature is 2−4 °C, and annual precipitation is 650 mm. There are, on average, 20−40 vascular plant species per 0.25 m^2. The vegetation is dominated by *Kobresia graminifolia*, *Poa botryoides*, *Elymus nutans*, and *Anemone rivularis*. The non-flooded Petri dish method (Foissner, 1987; Foissner, Agatha, & Berger, 2002) was used to stimulate ciliates to emerge from the soil samples. Ciliates were isolated and cultures were established at room temperature (*c*. 24 °C) in Petri dishes containing distilled water as a raw culture with squeezed rice grains to enrich the availability of bacterial food. Other hypotrichs such as *Oxytricha granulifera*, *Urosoma caudata*, *Urosoma macrostyla* and *Urosoma karinae sinense*, were found in same sampling.

Morphological observations were from specimens of raw soil percolate, that is, not from cloned individuals. Subsequently, when we collected cells for the DNA extraction, it cannot be excluded that similar species were mixed, although this is very unlikely because specimens which deviated in at least one important living morphological character were excluded. Furthermore, *Sterkiella sinica* sp. nov. was collected and rinsed four times with sterile water to remove other protists. So, we are sure that all data deal with this species.

Rubrioxytricha tsinlingensis sp. nov. was isolated from a freshwater pond in the northern part of the Tsinling Mountains, south-west of Xi'an (33 °46′N, 108 °28′E), China, in April 2013 when the water temperature was 7 °C and the pH measured 7.5. The Tsinling Mountains (maximum elevation 3,700 m) comprise the northernmost strip of transverse ranges that separate the Sichuan Basin from the steppes and plains of north-central China. The annual precipitation is about 850−950 mm although it declines to 700 mm in some areas. The vegetation is dominated by *Quercus acutissima*, *Ulmus* spp., *Juglans regia* and *Fraxinus* spp. Samples from the surface layer of the water (*c*. 0−10 cm) were collected and transferred to Petri dishes and assumed to belong to a single population, then maintained in the laboratory with water *in situ* for several days at room temperature (*c*. 24 °C) as a raw culture for further studies. A few wheat grains were added to support the growth of bacteria, besides diatoms as important food for our *Rubrioxytricha* population.

Unfortunately, we could not establish a clone and therefore we cannot be 100% sure that the specimens used for the morphological studies and molecular analyses belong to the same species. However, as no other *Rubrioxytricha* morphotypes have been present in the protargol preparations, the probability is extremely high that our morphological and molecular studies deal with the same species.

Observation of morphology

Living cells were observed using bright field and differential interference contrast microscopy at 100−1000×. Protargol staining (Wilbert, 1975) was used to reveal the infraciliature and nuclear apparatus. Counts and measurements of stained specimens were performed with an ocular micrometer. Drawings were made with the help of a camera lucida. Terminology, numbering system for cirri, and systematics are according to Berger (1999).

DNA extraction, PCR amplification, and sequencing

Extraction of genomic DNA was performed using a DNeasy Blood & Tissue Kit (Qiagen, Hilden, Germany), following the manufacturer's instructions. The SSU rRNA genes were amplified using universal primers Eukaryotic A (5′-AAC CTG GTT GAT CCT GCC AGT-3′) and Eukaryotic B (5′-TGA TCC TTC TGC AGG TTC ACC TAC-3′) (Medlin, Elwood, Stickel, & Sogin, 1988). Cloning and sequencing were performed according to previous procedures (Huang, Chen, Song, & Berger 2014).

Sequencing and phylogenetic analyses

We included their SSU rRNA sequences and those of 69 other taxa obtained from the GenBank database (see Fig. 35 for accession numbers except those of the

following 13 urostylids: *Anteholosticha pseudomonilata* HM568416, *Heterokeronopsis pulchra* JQ083600, *Nothoholosticha fasciola* FJ377548, *Pseudokeronopsis carnae* AY881633, *Uroleptopsis citrina* GU437211, *Pseudourostyla cristata* GU942569, *Hemicycliostyla sphagni* FJ361758, *Monocoronella carnea* FJ775726, *Diaxonella trimarginata* DQ190950, *Urostyla grandis* EF535731, *Apokeronopsis wrighti* EU417963, *Thigmokeronopsis stoecki* EU220226 and *Metaurostylopsis salina* EU220229) in phylogenetic analyses. Four species of the subclasses Oligotrichia and Choreotrichia were chosen as the outgroup taxa. Sequences were aligned on the web server GUIDANCE using MUSCLE with the alignment algorithm and the default parameters (Penn et al., 2010). Both ends of the alignments were trimmed before further analysis. The final alignment, including 1702 sites and 71 taxa, was used to construct phylogenetic trees. The Bayesian inference (BI) analysis was performed with MrBayes v.3.2.5 (Ronquist & Huelsenbeck, 2003) using GTR + *I* + *G* as the best model selected by MrModeltest v.2.3 (Nylander, 2004) under the Akaike Information Criterion. Two Markov Chain Monte Carlo (MCMC) simulations were run for 10,000,000 generations with a sampling frequency of every 100 generations and a burn-in of 25,000 trees (25%). Maximum-likelihood (ML) trees were constructed on the CIPRES Science Gateway using RAxML-HPC2 on XSEDE v8.2.4 (Stamatakis, 2014) with 1000 bootstrap replicates. Tree topologies were visualized in MEGA 6.0 (Tamura, Stecher, Peterson, Filipski, & Kumar, 2013).

Results

Class Spirotrichea Bütschli, 1889
Subclass Hypotrichia Stein, 1859
Order Sporadotrichida Fauré-Fremiet, 1961
Family Oxytrichidae Ehrenberg, 1838
Genus: *Sterkiella* Foissner, Blatterer, Berger & Kohmann, 1991

Sterkiella sinica sp. nov.
(Figs 5–19; Table 1)

Diagnosis. Body elongate oval to elliptical, measuring 85–110 × 35–45 μm *in vivo*. Two macronuclear nodules and two to five micronuclei. Pellicle rigid. One contractile vacuole located approximately at mid-body. *C.* 28 membranelles. Invariably 18 frontoventral transverse cirri, cirrus III/2 anteriad of cirrus IV/3 and closer to cirrus IV/3 than to paroral, cirrus V/3 closer to cirrus V/4 than to cirrus V/2, cirrus V/2 closer to cirrus VI/2 than to cirrus V/3. Marginal rows normally confluent posteriorly. Six dorsal kineties and three relatively inconspicuous and narrowly separated caudal cirri. Soil habitat.

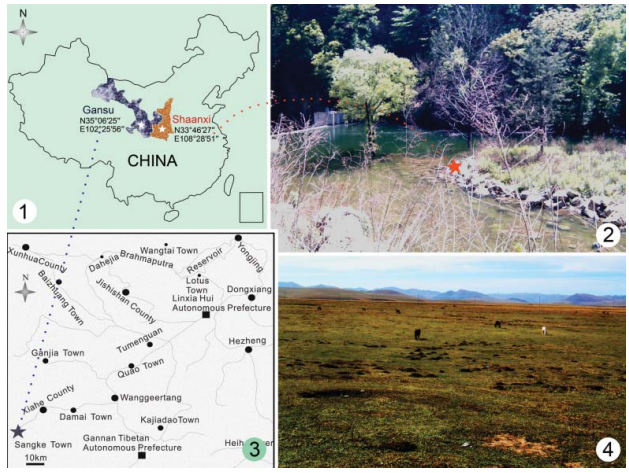

Fig. 1–4. Sample sites and surrounding areas. (1) Map showing the locations of the northern part of the Tsinling Mountains, Shaanxi Province and Sangke Grassland, Gansu Province. (2) Location where *Rubrioxytricha tsinlingensis* sp. nov. was collected; (3, 4) location where *Sterkiella sinica* sp. nov. was collected.

Type locality. Collected from the surface soil in the Sangke Grass Land (35 °06′N, 102 °25′E), Gansu Province, China.

Type material. A protargol slide (no. CLY2011071501/A) with the holotype specimen (Figs 9, 10) marked and two paratype slides (nos CLY2011071501/B, C) have been deposited in the Laboratory of Protozoology, Ocean University of China. An additional paratype slide (registry no. NHMUK 2015.8.28.2) has been deposited in the

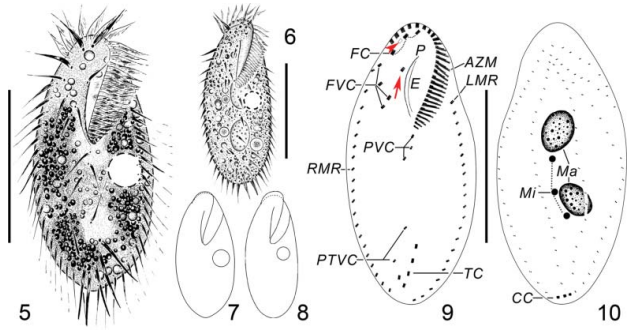

Fig. 5–10. Morphology of *Sterkiella sinica* sp. nov. from life (5–8) and after staining with protargol (9, 10); (5) Ventral view of a representative individual; (6–8) Ventral views of other individuals showing different body shapes; (9, 10) Infraciliature of ventral and dorsal sides and macronuclear apparatus of holotype specimen; arrow indicates the buccal cirrus, arrowhead marks the extra cirrus. AZM, adoral zone of membranelles; CC, caudal cirri; E, endoral; FC, frontal cirri; FVC, frontoventral cirri; LMR, left marginal row; Ma, macronuclear nodules; Mi, micronuclei; P, paroral; PTVC, pretransverse ventral cirri; PVC, postoral ventral cirri; RMR, right marginal row; TC, transverse cirri. Scale bars: 65 μm.

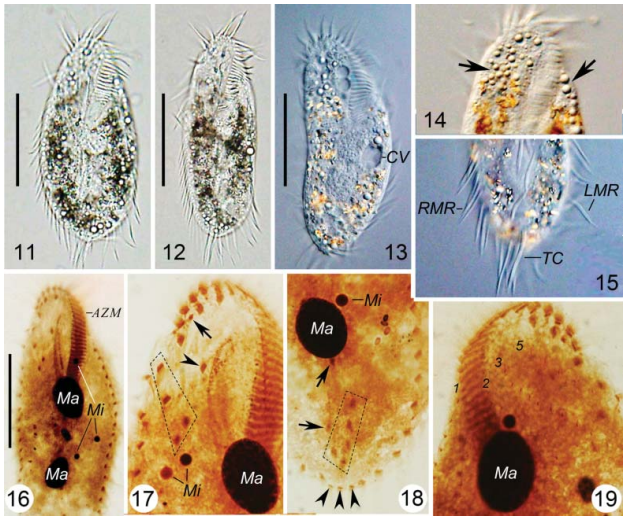

Fig. 11–19. Photomicrographs of *Sterkiella sinica* sp. nov. from life (11–15) and after staining with protargol (16–19); (11) Ventral view of a typical cell; (12, 13) Ventral views of different individuals, squeezed cells showing in Fig. 13; (14) Ventral view of the anterior portion showing refringent cytoplasmic globules (arrows); (15) Ventral view of the end of the cell showing transverse cirri and the strong marginal cirri on both left and right sides; (16, 17) Ventral views showing the nuclear apparatus and frontal, buccal (arrowhead), and frontoventral cirri (in trapezoid). Arrow indicates the extra cirrus; (18) Ventral view of the posterior portion of cell showing the pretransverse ventral (arrows), transverse (in trapezoid), and caudal cirri (arrowheads); (19) Dorsal view showing the dorsal kineties. AZM, adoral zone of membranelles; CV, contractile vacuole; LMR, left marginal row; Ma, macronuclear nodules; Mi, micronuclei; RMR, right marginal row; TC, transverse cirri; 1–3, 5, dorsal kineties. Scale bars: 50 μm.

Natural History Museum UK. All slides are protargol preparations.

Etymology. The specific epithet refers to its place of discovery.

Description. Cells *in vivo* measuring 85–110 × 35–45 μm, usually elongate oval to elliptical in shape, with anterior end narrowly rounded and posterior end broadly rounded (Figs 5–8, 11–12). Pellicle rigid. Cells colourless to grey; cytoplasm colourless, containing several food vacuoles filled with bacteria and diatoms, refringent cytoplasmic crystals, and granules measuring 1–4 μm in diameter (Fig. 14). Cortical granules absent. Contractile vacuole 15–20 μm in diameter, located in mid-body region near left margin and discharging at intervals of 4 s (Figs 5–8, 13). Two ellipsoidal macronuclear nodules, each measuring *c*. 40 μm × 20 μm, located at mid-body near the mid-line and containing many spherical nucleoli (Figs 10, 16–19). Two to five micronuclei. Locomotion is by running moderately quickly on debris.

Infraciliature as shown in Figs 9, 10, 16–19. Buccal field/length of body *c*. 40% *in vivo* (*c*. 38% after fixation and staining) (Figs 5, 6, 11–13). Adoral zone composed of 25–30 membranelles (average 28). Bases of largest membranelles *c*. 10 μm wide, cilia up to 15 μm long. Distal portion of adoral zone extends slightly posteriorly onto right side of cell, with a DE-value of 0.17 in the holotype specimen (Fig. 9; for explanation of DE-value, see Berger 2006: 18). Endoral and paroral optically parallel, both bending slightly toward left; paroral slightly longer than endoral (Figs 9, 16). Frontoventral transverse ciliature comprising 18 cirri. Three slightly enlarged frontal cirri with cilia *c*. 18 μm long. One extra frontal cirrus present in five of 11 specimens examined, located rightward of middle frontal cirrus (cirrus II/3). Single buccal cirrus near anterior end of paroral. Frontoventral cirri arranged in a short, mixed, asymmetric, V-shaped row; cirrus III/2 anteriad of cirrus IV/3 and closer to cirrus IV/3 than to paroral (Figs 9, 16, 17). Three postoral ventral cirri located behind buccal vertex, with cirrus IV/2 arranged anterior to cirrus V/4 (Fig. 9); distance between cirri V/3 and V/4 much shorter than that between cirri V/3 and V/2. Five transverse cirri in hook-shaped pseudo-row and not forming two distinct groups, with cilia *c*. 20 μm long (Figs 9, 18). Two fine pretransverse ventral cirri close to transverse cirri, cirrus VI/2 located near rightmost transverse cirrus, cirrus V/2 closer to cirrus VI/2 than cirrus V/3. One right and one left marginal row, posterior ends of which are normally separated; left row with 19–23 cirri, right row with 18–22 cirri; cilia of marginal cirri *c*. 15 μm long.

Six dorsal kineties: leftmost two (dorsal kineties 1 and 2) bipolar, comprising 22–25 and 20–24 dikinetids, respectively; dorsal kinety 3 starts at level 1/6 of length of cell from anterior end, slightly shortened posterior end, composed of 14–19 dikinetids; dorsal kinety 4 comprising 13–19 dikinetids originating 1/5 of length of cell from anterior end and extending to posterior end of cell; rightmost two dorsal kineties (= dorsomarginal kineties) originate near anterior end of cell, with dorsal kinety 5 terminating at 1/3 of length of cell from anterior end and usually composed of 9–15 dikinetids and dorsal kinety 6 terminating at 25% of length of cell from anterior and usually composed of 5–10 dikinetids (Figs 10, 19). Dorsal cilia *c*. 3 μm long *in vivo*. Three caudal cirri located at posterior body margin, narrowly separated, one each at posterior end of dorsal kineties 1, 2, and 4; cilia of caudal cirri *c*.15 μm long *in vivo* (Figs 10, 18).

Genus *Rubrioxytricha* Berger, 1999

Rubrioxytricha tsinlingensis sp. nov.
(Figs 20–34; Table 1)

Diagnosis. Body elongate, measuring 100–180 μm × 35–60 μm *in vivo* and yellow-brown in colour. Two

Table 1. Morphological characterization of *Sterkiella sinica* sp. nov. (upper line) and *Rubrioxytricha qinlingi* sp. nov. (lower line).

Character [a]	HT	Min	Max	Mean	SD	CV	*n*
Length of body	115	98	131	114.4	10.04	8.8	11
	145	144	186	161.3	12.57	7.8	15
Width	54	43	61	54.1	6.56	12.1	11
	63	64	89	73.4	7.11	9.7	15
Length of adoral zone	43	39	46	43.6	2.01	4.6	11
	49	44	56	47.7	3.10	6.5	15
Number of adoral membranelles	29	25	30	28.1	1.64	5.8	11
	38	36	44	38.3	2.16	5.6	15
Number of buccal cirri	1	1	1	1.0	0	0	11
	1	1	1	1.0	0	0	15
Number of frontal cirri	3	3	3	3.0	0	0	11
	3	3	3	3.0	0	0	15
Number of frontoventral cirri	4	4	4	4.0	0	0	11
	4	4	4	4.0	0	0	15
Number of postoral ventral cirri	3	3	3	3.0	0	0	11
	3	3	3	3.0	0	0	15
Number of pretransverse cirri	2	2	2	2.0	0	0	11
	2	2	2	2.0	0	0	15
Number of transverse cirri	5	5	5	5.0	0	0	11
	5	5	5	5.0	0	0	15
Number of caudal cirri	3	3	3	3.0	0	0	11
	3	3	3	3.0	0	0	15
Number of left marginal cirri	21	19	23	20.7	1.42	6.9	11
	35	28	40	35.1	2.95	8.4	15
Number of right marginal cirri	20	18	22	20.2	1.17	5.8	11
	34	32	38	34.4	1.84	5.4	15
Number of dorsal kineties	6	6	6	6.0	0	0	11
	6	6	6	6.0	0	0	15
Number of basal bodies in dorsal kinety 1	25	22	25	23.7	1.10	4.7	11
	24	22	25	23.8	1.01	4.3	15
Number of basal bodies in dorsal kinety 2	22	20	24	22.3	1.42	6.4	11
	25	23	26	24.7	0.90	3.6	15
Number of basal bodies in dorsal kinety 3	18	14	19	15.9	1.38	8.6	11
	25	22	25	23.9	1.13	4.7	15
Number of basal bodies in dorsal kinety 4	19	13	19	16.0	2.05	12.8	11
	16	13	17	15.3	1.40	9.1	15
Number of basal bodies in dorsal kinety 5	9	9	15	12.4	2.42	19.6	11
	27	24	29	26.4	1.40	5.3	15
Number of basal bodies in dorsal kinety 6	6	5	10	6.9	1.70	24.6	11
	7	5	9	6.7	1.10	16.3	15
Distance between cirrus III/2 and undulating membranes	6.7	5.5	8.6	6.2	0.90	14.4	11
	3.6	3.2	4.0	3.5	0.23	6.6	15
Distance between cirri III/2 and IV/3	4.4	4.0	4.8	4.5	0.30	6.7	11
	3.7	3.4	3.8	3.6	0.12	3.4	15
Distance between cirri V/2 and V/3	29.0	17.8	29.0	24.5	3.74	15.2	11
	49.9	47.1	52.3	49.4	1.27	2.6	15
Distance between cirri V/2 and VI/2	12.0	11.5	16.4	13.4	1.53	11.4	11
	8.9	7.7	9.3	8.4	0.58	6.9	15
Distance between cirri V/3 and V/4	5.5	5.3	8	6.7	0.73	10.9	11
	7.9	7.1	8.5	7.7	0.45	5.8	15
Number of macronuclear nodules	2	2	2	2.0	0	0	11
	2	2	2	2.0	0	0	15
Number of micronuclei	3	2	5	2.8	0.87	31.0	11
	2	2	3	2.1	0.26	12.5	15

[a]All data are based on protargol-stained specimens. All measurements in μm. Abbreviations: CV, coefficient of variation in %; HT, holotype; Max, maximum; Mean, arithmetic mean; Min, minimum; *n*, number; SD, standard deviation.

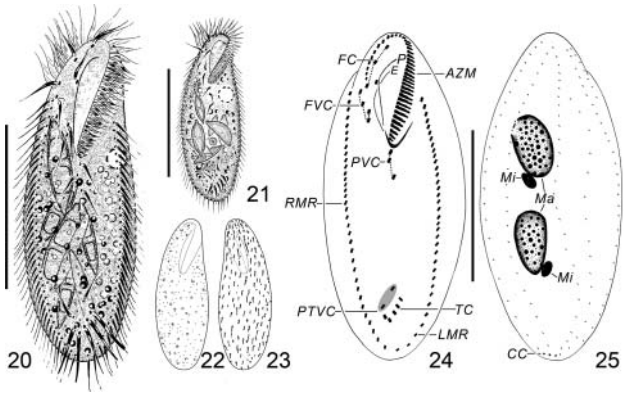

Fig. 20–25. Morphology of *Rubrioxytricha tsinlingensis* sp. nov. from life (20–23) and after staining with protargol (24, 25); (20) Ventral view of a typical cell; (21) Ventral view of different individual; (22, 23) Ventral and dorsal sides, showing the distribution of the cortical granules; (24, 25) Infraciliature of ventral and dorsal sides and nuclear apparatus of holotype specimen. AZM, adoral zone of membranelles; CC, caudal cirri; E, endoral; FC, frontal cirri; FVC, frontoventral cirri; LMR, left marginal row; Ma, macronuclear nodules; Mi, micronuclei; P, paroral; PTVC, pretransverse ventral cirri; PVC, postoral ventral cirri; RMR, right marginal row; TC, transverse cirri. Scale bars: 85 μm.

macronuclear nodules and two or three micronuclei. Cortical granules yellow-green, densely grouped in clusters on ventral side and irregular short rows on dorsal side. One contractile vacuole located *c*. 1/3 of body length. *C.* 38 membranelles. Invariably 18 frontoventral transverse cirri. Marginal rows almost confluent posteriorly. Six dorsal kineties and three caudal cirri. Caudal cirri and dorsal bristles almost indistinguishable when viewed *in vivo*. Freshwater habitat.

Type locality. China, Shaanxi Province; freshwater pond in the northern part of Tsinling Mountains southwest of Xi'an (33 °46′N, 108 °28′E).

Type material. A protargol slide (registry no. CLY2013042003/A) with the holotype specimen (Figs 24, 25) marked and three paratype slides (nos CLY2013042003/B-D) have been deposited in the collection of the Laboratory of Protozoology, Ocean University of China, China. An additional paratype slide (registry no. NHMUK 2015.8.28.1) has been deposited in the collection of the Museum of Natural History UK. All slides are protargol preparations.

Etymology. The specific epithet *tsinlingensis* refers to the geographic location where the type specimens were discovered.

Description. Body measuring 100–180 μm × 35–60 μm *in vivo*, length/width *c*. 3:1 *in vivo*, 2.2:1 on average in fixed and stained cells. Non-contractile and flexible, usually slender oval to elliptical with anterior end usually narrow, posterior broadly rounded; left margin slightly convex, right margin strongly convex in typical individuals (Figs 20, 21, 26, 27). Dorsoventrally flattened (*c*. 3:1), ventral side flat, dorsal side convex in middle portion. Body yellow-brown when observed at low magnifications. Cytoplasm slightly brown, containing numerous refringent globules and crystals. Cells typically filled with food vacuoles containing green algae on average *c*. 2–4 μm across, rounded and elongate (measuring *c*. 40 μm × 5μm) diatoms, and bacteria. (Figs 30, 32). Cortical granules yellow-green, spherical, *c*. 0.5 μm in diameter, arranged in slightly sparse clusters on ventral side and irregular short rows on dorsal surface (Figs 22, 23, 29). Contractile vacuole *c*. 20 μm in diameter with fully extended, located *c*. 1/3 of body length from anterior end near left cell margin, discharging at intervals of *c*. 8–10 s (Figs 20, 21, 28). Macronuclear nodules, measuring *c*. 20 μm × 14 μm *in vivo*, spherical to ellipsoidal, usually arranged in a line at midbody and slightly left of midline, with small to moderately large nucleoli (Figs 25, 30). Each macronuclear nodule usually with one micronucleus located nearby (Fig. 25). Locomotion by continuous, rapid running on bottom of Petri dish and surface film of water. Cells often swim continuously in circles when free from surfaces.

Infraciliature as shown in Figs 24, 25, 31–34. Adoral zone occupies 30–35% of cell length *in vivo* (*c*. 30% after fixation and staining), composed of 36–44 membranelles. Bases of largest adoral membranelles *c*. 10 μm wide, cilia up to 15 μm long (Figs 24, 31). Distal portion of adoral zone extends far down right side of cell, that is, DE-value 0.43 in holotype specimen (Fig. 24). Paroral and endoral intersect in optical section at level of the buccal cirrus (Figs 24, 31). Frontoventral transverse ciliature comprising 18 cirri: three slightly enlarged frontal cirri with cilia *c*. 15 μm long; single buccal cirrus near intersection of paroral and endoral; frontoventral cirri arranged in a short, mixed, asymmetric, V-shaped row; cirrus III/2 slightly anteriad of cirrus IV/3, and distance between cirri III/2 and IV/3 equal to that between cirri III/2 and endoral; three postoral ventral cirri located medially below vertex and distinctly separated from the two pre-transverse ventral cirri; cirrus IV/2 arranged anteriorly than cirrus V/4; five transverse cirri arranged roughly in a J-shaped pseudo-row in posterior region of cell, with cilia *c*. 25 μm long (Figs 20, 24, 31–34). One right and one left marginal row, posterior ends of which are almost confluent; left row with 28–40 cirri, right row with 32–38 cirri; cilia of marginal cirri *c*. 10 μm long (Figs 24, 32).

Six dorsal kineties; dorsal kineties 1–3 and 5 almost bipolar, comprising 22–25, 23–26, 22–25, 24–29 dikinetids, respectively; dorsal kinety 4 originates at level near 1/5 of body length from anterior end of cell and

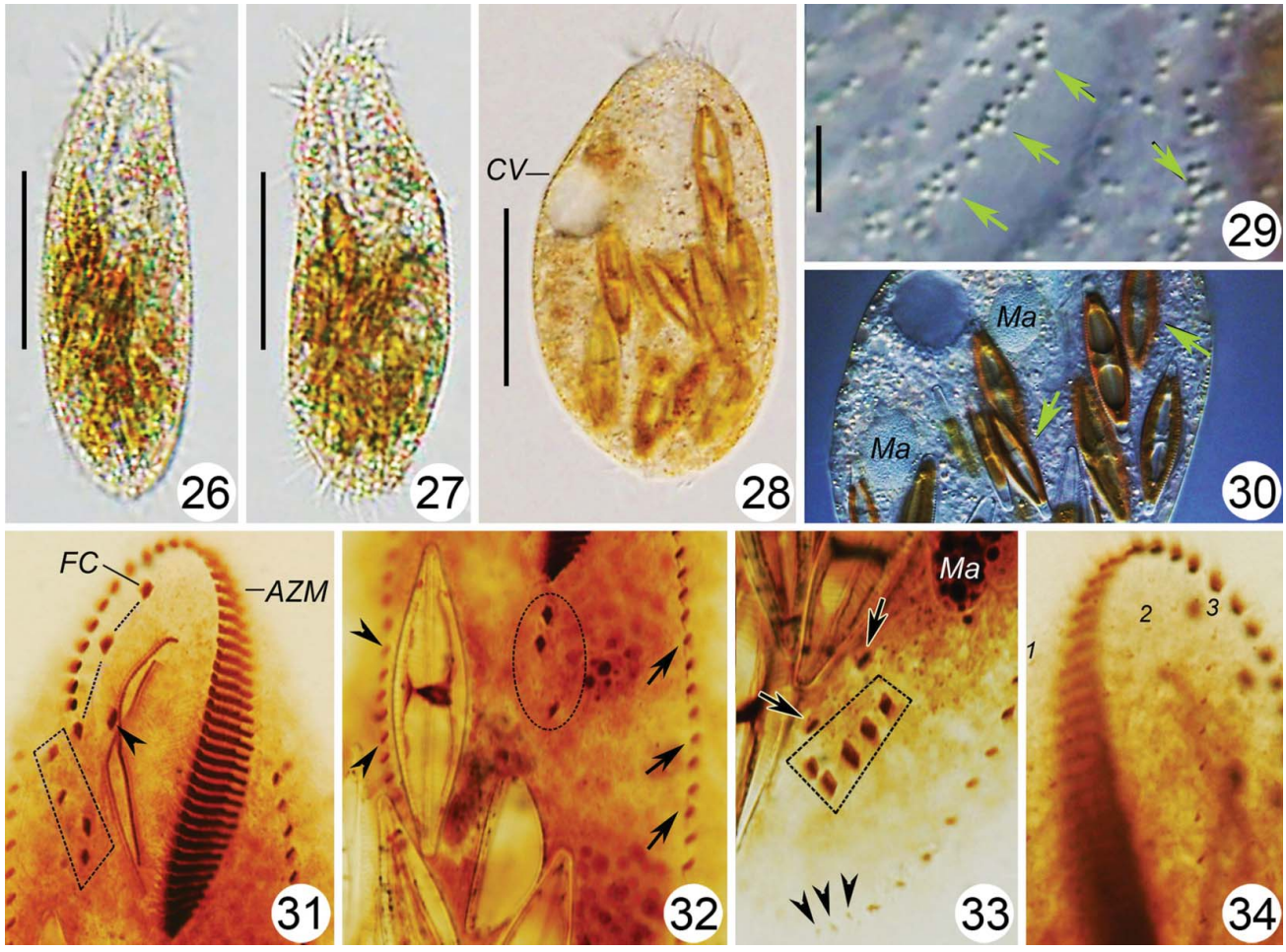

Fig. 26–34. Photomicrographs of *Rubrioxytricha tsinlingensis* sp. nov. from life (26–30) and after staining with protargol (31–34); (11) Ventral view of a typical cell. (27, 28) Ventral and dorsal views of different individuals, squeezed cells showing in Fig. 28; (29, 30) Dorsal views, to show the arrangement of the cortical granules (arrows in Fig. 29) and diatoms (*Navicula* sp.) (arrows in Fig. 30); (31) Ventral view of the anterior portion showing the frontal, buccal (arrowhead), frontoventral cirri (in trapezoid); (32) Ventral view of the middle portion of a cell showing the postoral ventral cirri (in circle), left (arrows) and right (arrowheads) marginal rows; (33) Ventral view of the posterior portion showing the pretransverse ventral (arrows), transverse (in trapezoid) and caudal cirri (arrowheads); (34) Dorsal view showing the dorsal kineties. AZM, adoral zone of membranelles; CV, contractile vacuole; FC, frontal cirri; Ma, macronuclear nodules; 1–3, dorsal kineties. Scale bars: Figs (26–28), 90 μm; Fig. (29), 4 μm.

extends to posterior end, comprising 13–17 dikinetids; rightmost dorsal kinety (dorsal kinety 6) composed of 5–9 dikinetids and originates at anterior end of cell (Figs 25, 34). Dorsal cilia *c*. 4 μm long *in vivo*. Three thin, caudal cirri located at posterior margin of body, narrowly separated, one each on dorsal kineties 1, 2, and 4 (Figs 25, 33); cilia of caudal cirri *c*. 12 μm long *in vivo* and thus of similar length to and almost indistinguishable from marginal cirri (Fig. 20).

Phylogenetic analysis (Fig. 35)

The SSU rRNA sequences of both new species have been deposited in GenBank and the lengths and accession numbers are as follows: *Sterkiella sinica* sp. nov. (1688 bp, KR817676) and *Rubrioxytricha tsinlingensis* sp. nov. (1628 bp, KR817675). The G + C contents of the two species are 44.79% and 45.45% respectively.

As the topologies of ML and BI trees were comparatively identical, here we present the ML tree with node supports from both methods (Fig. 35). The family Oxytrichidae is found to be polyphyletic, which is consistent with previous studies (Jung, Park, & Min, 2015; Kumar, Bharti, Marinsalti, Insom, & Terza, 2014; Schmidt, Bernhard, Schlegel, & Foissner, 2007; Singh & Kamra, 2015b). The monophyly of the subfamily Stylonychinae is well supported when the newly sequenced *Sterkiella sinica* sp. nov. was added, which supports the assertion that a rigid pellicle without cortical granules is a synapomorphy (Berger & Foissner, 1997).

The genus *Sterkiella* was assigned into the subfamily Stylonychinae in Berger's work (1999). In the present

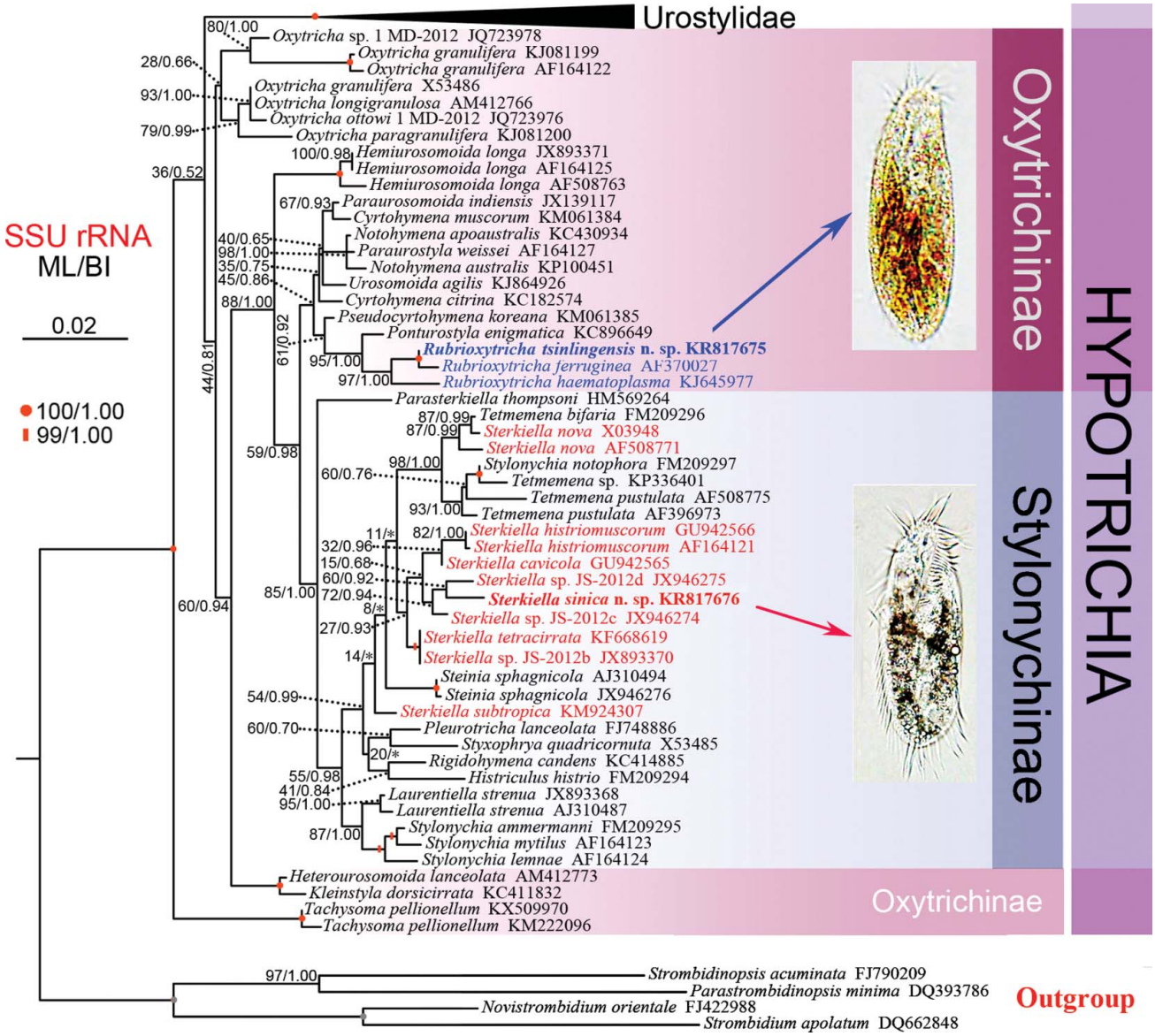

Fig. 35. Maximum likelihood (ML) phylogenetic tree inferred from the small subunit rRNA (SSU rRNA) gene sequences of 60 hypotrichs showing the positions of *Rubrioxytricha tsinlingensis* sp. nov. and *Sterkiella sinica* sp. nov. Numbers at the nodes represent the bootstrap values of ML analyses and posterior probability of BI analyses. Asterisk (*) represents support values less than 50% and the disagreement between the reference the ML and the BI tree. The scale bar corresponds to two substitutions per 100 nucleotide positions. The newly sequenced species in the present study are shown in bold.

analysis, the newly sequenced *Sterkiella sinica* sp. nov. does not branch with all the other *Sterkiella* species in a monophyletic assemblage as expected (Fig. 35). Instead, it clusters with seven species of *Sterkiella* (GenBank nos GU942566, AF164121, GU942565, JX946275, JX946274, KF668619, JX893370) with rather low support (27%ML, 0.93BI), indicating that this relationship is far from robust. Additionally, another two sequences of *S. nova* cluster with *Tetmemena bifaria*, yet *S. subtropica* occupies a basal position with another group comprising two sequences of *Steinia sphagnicola* (Fig. 35). The relationship among the genus *Sterkiella* is not clear in present and previous studies: the topology is not stable and the support values are not high (Chen et al., 2015; Kumar et al., 2015).

Rubrioxytricha tsinlingensis sp. nov. clusters with the other two *Rubrioxytricha* species (*Rubrioxytricha ferruginea* and *Rubrioxytricha haematoplasma*) with high support values (97% ML, 1.00 BI), which are consistent with morphology (e.g., homogeneously coloured cytoplasm and flexible body from the living cell). The highly stable monophyly of the genus *Rubriosytricha* were also supported in previous phylogenetic analyses (Chen et al., 2015).

Table 2. Morphological and morphometric comparisons of four species of *Sterkiella*.

Character	*S. sinica*	*S. subtropica*	*S. histriomuscorum*	*S. tricirrata*
Length of body[a] (μm)	85−110	100−200	80−180	80
Width of body[a] (μm)	35−45	35−70	40−70	–
DE-value[b]	0.17	0.26[c]	0.16−0.21[c]	0.18[c]
Body shape	Elongate oval to elliptical, anterior end narrowly rounded and posterior end broadly rounded	Fusiform to teardrop-shaped with posterior obviously wider than anterior	Body margins parallel, both ends rounded	Elliptical
Adoral membranelles, number	25−30	25−39	26−44	23−25
Transverse cirri, number	5	5	3−6	3
Left marginal cirri, number	19−23	18−26	12−25	10−13[c]
Right marginal cirri, number	18−22	19−27	17−32	11−13[c]
Dorsal kineties, number	6	6	6−7	5 or 6
Number of dikinetids in DK1,	22−25	21[c]	16−28	–
Number of dikinetids in DK2	20−24	18[c]	17−26	–
Number of dikinetids in DK3	14−19	16[c]	11−19	–
Number of dikinetids in DK4	13−19	13[c]	7−19	–
Number of dikinetids in DK5	9−15	10[c]	6−14	–
Number of dikinetids in DK6	5−10	4[c]	2−7	–
Macronuclear nodules, number	2	2	2	–
Micronuclei, number	2−5	1−4	1−3	2
Habitat	Terrestrial	Mangrove mud, covered with marine water	Terrestrial and freshwater	Terrestrial
Source of data	Present work	Chen et al. (2015)	Berger (1999)	Berger (1999)

[a]In living cells.
[b]Indicates the distance between anterior body end and distal end of AZM divided by length of AZM (Berger, 2006).
[c]Data for drawing. Abbreviations: DK1−6, dorsal kineties.

Discussion

Comparison of *Sterkiella sinica* sp. nov. with similar species

In terms of its two macronuclear nodules, three nominal congeners, namely *Sterkiella subtropica* Chen et al., 2015, *S. histriomuscorum* (Foissner, Blatterer, Berger & Kohmann, 1991) and *S. tricirrata* (Buitkamp, 1977) Berger, 1999 should be compared with *S. sinica* sp. nov. (Berger, 1999; Chen et al., 2015).

According to the most recent report, *Sterkiella sinica* sp. nov. is very similar to *S. subtropica* Chen et al., 2015. The former differs from the latter in having less body length *in vivo* (85−110 μm vs. 100−200 μm); cirrus V/3 closer to cirrus V/4 (vs. cirrus V/2) and different habitat (terrestrial vs. mud covered with marine water) (Chen et al., 2015).

Sterkiella sinica sp. nov. can be separated from *S. histriomuscorum* by: (1) position of cirrus V/3 (closer to V/4 vs. same distance with V/4 and V/2); (2) transverse cirri in asymmetry V vs. hook shape) (Berger, 1999). Moreover, the sequence data strongly indicates that the two forms belong to clearly different species (Fig. 35).

Sterkiella sinica sp. nov. differs from *S. tricirrata* in the number of transverse cirri (5 vs. 3), left (19−23 vs. 10−13) and right (18−22 vs. 11−13) marginal cirri (data from drawing, Berger, 1999).

For comparative purposes, details of the main morphological features of these taxa are given in Table 2.

Comparison of *Rubrioxytricha tsinlingensis* sp. nov. with similar species

Currently, three morphospecies are assigned to the genus *Rubrioxytricha*: *R. haematoplasma* (Blatterer & Foissner, 1990) Berger, 1999, *R. ferruginea* (Stein, 1859) Berger, 1999 and *R. indica* Naqvi, Gupta, Borgohain, & Sapra, 2006 (Berger, 1999; Naqvi, Gupta, Borgohain, & Sapra, 2006).

Considering its somatic ciliature, *R. tsinlingensis* sp. nov. is most similar to *R. ferruginea*, although the former differs from the latter in colour of cell (yellow-brown vs. intense rusty) and cortical granules (yellow-green vs. brown or brownish) and number of dorsal kineties (6 vs. 5) and caudal cirri (3 vs. 1 or 2) (Berger, 1999).

Rubrioxytricha tsinlingensis sp. nov. can be distinguished from *R. haematoplasma* by having yellow-brown (vs. red to ash-black) cell colour, yellow-green (vs. orange-red) cortical granules, 3 (vs. 1) caudal cirri, 6 (vs.

4) dorsal kineties, freshwater (vs. brackish) habitat (Berger, 1999; Chen, Chen, Li, Warren, & Lin, 2015).

Compared with *Rubrioxytricha tsinlingensis* sp. nov., *R. indica* has dark green (vs. yellow-green) cortical granules, a smaller body size *in vivo* (80 × 30 μm vs. 100−180 μm × 35−60 μm), three (vs. one) contractile vacuoles, fewer adoral membranelles (27−31 vs. 36−44), left (17−21 vs. 28−40) and right (21−24 vs. 32−38) marginal cirri, caudal cirri (1 vs. 3) and dorsal kineties (5 vs. 6) (Naqvi et al., 2006).

Acknowledgements

This work was supported by the National Natural Science Foundation of China (project numbers: 31372148), Scientific and Technological Coordination and Innovation Project of Shaanxi Province (No2015KTTSNY01-07), Science Foundation of the Chinese Academy of Sciences Project (Y55201CY00), and the China Scholarship Council, which funded an extended visit by the principal author to North Carolina Central University, USA. Our thanks are also due to Prof. Weibo Song for constructive suggestions and Mr Ping Li, for collecting the sample.

Disclosure statement

No potential conflict of interest was reported by the authors.

Funding

This work was supported by the National Natural Science Foundation of China [project numbers: 31372148]; Scientific and Technological Coordination and Innovation Project of Shaanxi Province [No 2015KTTSNY01-07], Science Foundation of the Chinese Academy of Sciences Project [Y55201CY00].

References

Berger, H. (1999). Monograph of the Oxytrichidae (Ciliophora, Hypotrichia). *Monographiae Biologicae, 78*, 1−1080.

Berger, H. (2006). Monograph of the Urostyloidea (Ciliophora, Hypotricha). *Monographiae Biologicae, 85*, 1−1301.

Berger, H. (2008). Monograph of the Amphisiellidae and Trachelostylidae (Ciliophora, Hypotrichida). *Monographiae Biologicae, 88*, 1−737.

Berger, H. (2011). Monograph of the Gonostomatidae and Kahliellidae (Ciliophora, Hypotricha). *Monographiae Biologicae, 90*, 1−741.

Berger, H., & Foissner, W. (1997). Cladistic relationships and generic characterization of oxytrichids hypotrichs (Protozoa, Ciliophora). *Archiv für Protistenkunde, 148*, 125−155. doi:10.1016/S0003-9365(97)80048-6

Bharti, D., Kumar, S., & Terza, A. L. (2015). Two gonostomatid ciliates from the soil of Lombardia, Italy; including note on the soil mapping project. *Journal of Eukaryotic Microbiology, 62*, 762−772. doi:10.1111/jeu.12234

Bourland, W. A. (2015). Morphology, ontogenesis and molecular characterization of *Atractos contortus* Vörösváry, 1950 and *Stichotricha aculeata* Wrzesniowskiego, 1866 (Ciliophora, Stichotrichida) with consideration of their systematic positions. *European Journal of Protistology, 51*, 351−373. doi:10.1016/j.ejop.2015.06.004

Chen, W., Chen, X., Li, L., Warren, A., & Lin, X. (2015). Morphology, morphogenesis and molecular phylogeny of an oxytrichid ciliate, *Rubrioxytricha haematoplasma* (Blatterer & Foissner, 1990) Berger, 1999 (Ciliophora, Hypotricha). *International Journal of Systematic and Evolutionary Microbiology, 65*, 309−320. doi:10.1099/ijs.0.067801-0

Chen, X. M., Gao, F., Al-Farraj, S. A., Al-Rasheid, K. A. S., Xu, K., & Song, W. (2015). Morphology and morphogenesis of a novel mangrove ciliate, *Sterkiella subtropica* sp. nov. (Protozoa, Ciliophora, Hypotrichia), with phylogenetic analyses based on small-subunit rDNA sequence data. *International Journal of Systematic and Evolutionary Microbiology, 65*, 2292−2303. doi:10.1099/ijs.0.000253

Chen, X. M., Huang, J., & Song, W. (2011). Ontogeny and phylogeny of *Metaurostylopsis cheni* spec. nov. (Protozoa, Ciliophora), with estimating the systematic position of *Metaurostylopsis*. *Zoologica Scripta, 40*, 99−111. doi:10.1111/j.1463-6409.2010.00451.x

Fan, Y., Lu, X., Huang, J., Hu, X., & Warren, A. (2016). Redescription of two little-known urostyloid ciliates, *Anteholosticha randani* (Grolière, 1975) Berger, 2003 and *A. antecirrata* Berger, 2006 (Ciliophora, Urostylida). *European Journal of Protistology, 53*, 96−108. doi:10.1016/j.ejop.2016.01.001

Fan, Y., Zhao, X., Hu, X., Miao, M., Warren, A., & Song, W. (2015). Taxonomy and molecular phylogeny of two novel ciliates, with establishment of a new genus, *Pseudogastrostyla* n. g. (Ciliophora, Hypotrichia, Oxytrichidae). *European Journal of Protistology, 51*, 374−385. doi:10.1016/j.ejop.2015.06.007

Foissner, W. (1987). Soil protozoa: Fundamental problems, ecological significance, adaptations in ciliates and testaceans, bioindicators, and guide to the literature. *Progress in Protistology, 2*, 69−212.

Foissner, W., Agatha, S., & Berger, H. (2002). Soil ciliates (Protozoa, Ciliophora) from Namibia (Southwest Africa), with emphasis on two contrasting environments, the Etosha region and the Namib Desert. Part I. Text and line drawings. *Denisia, 5*, 1−1459.

Foissner, W., Blatterer, H., Berger, H., & Kohmann, F. (1991). Taxonomische und ökologische Revision der Ciliaten des Saprobiensystems. Band I: Cyrtophorida, Oligotrichida, Hypotrichia, Colpodea. *Informationsberichte des Bayerischen Landesamtes für Wasserwirtschaft, 1/91*, 1−478.

Gao, F., Warren, A., Zhang, Q., Gong, J., Miao, M., Sun, P., Xu, D., Huang, J., Yi, Z., & Song, W. (2016). The all-data-based evolutionary hypothesis of ciliated protists with a revised classification of the phylum Ciliophora (Eukaryota, Alveolata). *Scientific Reports, 6*, 24874. doi:10.1038/srep24874

Gao, F., Yi, Z., Gong, J., Al-Rasheid, K. A. S., & Song, W. (2010). Molecular phylogeny and species separation of five morphologically similar *Holosticha*-complex ciliates (Protozoa, Ciliophora) using ARDRA riboprinting and multigene sequence data. *Chinese Journal of Oceanology and Limnology, 28*, 542−548. doi:10.1007/s00343-010-9042-1

Hu, X., & Kusuoka, Y. (2015). Two oxytrichids from the ancient Lake Biwa, Japan, with notes on morphogenesis in

Notohymena australis (Ciliophora, Sporadotrichida). *Acta Protozoologica, 54*, 107−122. doi:10.4467/16890027AP.15.009.2734

Huang, J., Chen, Z., Song, W., & Berger, H. (2014). Three-gene based phylogeny of the Urostyloidea (Protista, Ciliophora, Hypotricha), with notes on classification of some core taxa. *Molecular Phylogenetics and Evolution, 70*, 337−347. doi:10.1016/j.ympev.2013.10.005

Huang, J., Yi, Z., Al-Farraj, S. A., & Song, W. (2010). Phylogenetic positions and taxonomic assignments of the systematically controversial genera, *Spirotrachelostyla*, *Uroleptopsis*, and *Tunicothrix* (Protozoa, Ciliophora, Hypotricha) based on small subunit rRNA gene sequences. *Systematics and Biodiversity, 8*, 409−416. doi:10.1080/14772000.2010.508502

Jung, J., Park, K., & Min, G. (2015). Morphology and molecular phylogeny of *Pseudocyrtohymena koreana* n. g., n. sp. and Antarctic *Neokeronopsis asiatica* Foissner *et al*., 2010 (Ciliophora, Sporadotrichida), with a brief discussion of the *Cyrtohymena* undulating membranes pattern. *Journal of Eukaryotic Microbiology, 62*, 280−297. doi:10.1111/jeu.12179

Kahl, A. (1932). Urtiere oder Protozoa I: Wimpertiere oder Ciliata (Infusoria) 3. Spirotricha. *Tierwelt Deutschlands Gustav Fischer, Jena, 25*, 399−650.

Kim, J. H., Vďačný, P., Shazib, S. U. A., & Shin, M. K. (2014). Morphology and molecular phylogeny of *Apoterritricha lutea* n. g., n. sp. (Ciliophora, Spirotrichea, Hypotrichia): A putative missing link connecting *Cyrtohymena* and *Afrokeronopsis*. *Journal of Eukaryotic Microbiology, 61*, 520−536. doi:10.1111/jeu.12131

Kumar, S., Bharti, D., Marinsalti, S., Insom, E., & Terza, A. L. (2014). Morphology, morphogenesis, and molecular phylogeny of *Paraparentocirrus sibillinensis* n. gen., n. sp., a "Stylonychine Oxytrichidae" (Ciliophora, Hypotrichida) without transverse cirri. *Journal of Eukaryotic Microbiology, 61*, 247−259. doi:10.1111/jeu.12103

Kumar, S., & Foissner, W. (2015). Biogeographic specializations of two large hypotrich ciliates: *Australocirrus shii* and *A. australis* and proposed synonymy of *Australocirrus* and *Cyrtohymenides*. *European Journal of Protistology, 51*, 210−228. doi:10.1016/j.ejop.2015.02.002

Kumar, S., Kamra, K., Bharti, D., Terza, A. L., Sehgal, N., Warren, A., & Sapra, G. R. (2015). Morphology, morphogenesis, and molecular phylogeny of *Sterkiella tetracirrata* n. sp. (Ciliophora, Oxytrichidae), from the Silent Valley National Park, India. *European Journal of Protistology, 51*, 86−97. doi:10.1016/j.ejop.2014.12.002

Li, J., Chen, X., & Xu, K. (2016). Morphology and small subunit rDNA phylogeny of two new marine urostylid ciliates, *Caudiholosticha marina* sp. nov. and *Nothoholosticha flava* sp. nov. (Ciliophora, Hypotrichia). *Journal of Eukaryotic Microbiology, 63*, 460−470. doi:10.1111/jeu.12290

Luo, X., Gao, F., Al-Rasheid, K. A. S., Warren, A., Hu, X., & Song, W. (2015). Redefinition of the hypotrichous ciliate *Uncinata*, with descriptions of the morphology and phylogeny of three urostylids (Protista, Ciliophora). *Systematics and Biodiversity, 13*, 455−471. doi:10.1080/14772000.2015.1046967

Lv, Z., Shao, C., Yi, Z., & Warren, A. (2015). A molecular phylogenetic investigation of *Bakuella*, *Anteholosticha*, and *Caudiholosticha* (Protista, Ciliophora, Hypotrichia) based on three-gene sequences. *Journal of Eukaryotic Microbiology, 62*, 391−399. doi:10.1111/jeu.12194

Medlin, L., Elwood, H. J., Stickel, S., & Sogin, M. L. (1988). The characterization of enzymatically amplified eukaryotic 16S-like rRNA-coding regions. *Gene, 71*, 491−499.

Naqvi, I., Gupta, R., Borgohain, P., & Sapra, G. R. (2006). Morphology and morphogenesis of *Rubrioxytricha indica* n. sp. (Ciliophora: Hypotrichida). *Acta Protozoologica, 45*, 53−64.

Nylander, J. A. (2004). *MrModeltest*. Sweden: Evolutionary Biology Centre, Uppsala University.

Paiva, T. D. S., Shao, C., Fernandes, N. M., Borges, B. D. N., & Silva-Neto, I. D. D. (2016). Description and phylogeny of *Urostyla grandis wiackowskii* subsp. nov. (Ciliophora, Hypotricha) from an estuarine mangrove in Brazil. *Journal of Eukaryotic Microbiology, 63*, 247−261. doi:10.1111/jeu.12273

Pan, X., Fan, Y., Gao, F., Qiu, Z., Al-Farraj, S. A., Warren, A., & Shao, C. (2016). Morphology and systematics of two freshwater urostylid ciliates, with description of a new species (Protista, Ciliophora, Hypotrichia). *European Journal of Protistology, 52*, 73−84. doi:10.1016/j.ejop.2015.11.003

Penn, O., Privman, E., Ashkenazy, H., Landan, G., Graur, D., & Pupko, T. (2010) GUIDANCE: A web server for assessing alignment confidence scores. *Nucleic Acids Research, 38*, W23−W28. doi:10.1093/nar/gkq443

Ronquist, F., & Huelsenbeck, J. P. (2003). MRBAYES 3: Bayesian phylogenetic inference under mixed models. *Bioinformatics, 19*, 1572−1574. doi:10.1093/bioinformatics/btg180

Schmidt, S. L., Bernhard, D., Schlegel, M., & Foissner, W. (2007). Phylogeny of the Stichotrichia (Ciliophora; Spirotrichea) reconstructed with nuclear small Subunit rRNA gene sequences: Discrepancies and accordances with morphological data. *Journal of Eukaryotic Microbiology, 54*, 201−209. doi:10.1111/j.1550-7408.2007.00250.x

Shao, C., Chen, L., Pan, Y., Warren, A., & Miao, M. (2014). Morphology and phylogenetic position of the oxytrichid ciliates, *Urosoma salmastra* (Dragesco and Dragesco-Kerneis, 1986) Berger, 1999 and *U. karinae sinense* nov. sp. (Ciliophora, Hypotrichia). *European Journal of Protistology, 50*, 593−605. doi:10.1016/j.ejop.2014.08.004

Singh, J., & Kamra, K. (2015a). Morphology and molecular phylogeny of an Indian population of *Cyrtohymena citrina* (Ciliophora, Hypotricha), including remarks on ontogenesis of *Urosomoida-Notohymena-Cyrtohymena* group. *European Journal of Protistology, 51*, 280−289. doi:10.1016/j.ejop.2015.06.002

Singh, J., & Kamra, K. (2015b). Molecular phylogeny of *Urosomoida agilis*, and new combinations: *Hemiurosomoida longa* gen. nov., comb. nov., and *Heterourosomoida lanceolata* gen. nov., comb. nov. (Ciliophora, Hypotricha). *European Journal of Protistology, 51*, 55−65. doi:10.1016/j.ejop.2014.11.005

Song, W., Warren, A., & Hu, X. (2009). *Free-living ciliates in the Bohai and Yellow Seas* (1st ed.). Beijing: Science Press.

Stamatakis, A. (2014). RAxML version 8: A tool for phylogenetic analysis and post-Analysis of large phylogenies. *Bioinformatics, 30*, 1312−1313. doi:10.1093/bioinformatics/btu033

Tamura, K., Stecher, G., Peterson, D., Filipski, A., & Kumar, S. (2013). MEGA6: Molecular Evolutionary Genetics Analysis version 6.0. *Molecular Biology and Evolution, 30*, 2725−2729. doi:10.1093/molbev/mst197

Wang, P., Gao, F., Huang, J., Strüeder-Kypke, M., & Yi, Z. (2015). A case study to estimate the applicability of secondary structures of SSU-rRNA gene in taxonomy and

phylogenetic analyses of ciliates. *Zoologica Scripta, 44*, 574−585. doi:10.1111/zsc.12122

Wilbert, N. (1975). Eine verbesserte Technik der Protargolimprägnation für Ciliaten. *Mikrokosmos, 64*, 171−179 (in German).

Yi, Z., Dunthorn, M., Song, W., & Stoeck, T. (2010). Increased taxon sampling using both unidentified environmental sequences and identified cultures for microbial eukaryotes improves phylogenetic inference. *Molecular Phylogenetics and Evolution, 57*, 937−941. doi:10.1016/j.ympev.2010.08.001

Yi, Z., Lin, X., Warren, A., Al-Rasheid, K. A. S., & Song, W. (2010) Molecular phylogeny of *Nothoholosticha* (Protozoa, Ciliophora, Urostylida) and systematic relationships of the *Holosticha*-complex. *Systematics and Biodiversity, 81*, 149−155. doi:10.1080/14772000903523493

Yi, Z., & Song, W. (2011). Evolution of the order Urostylida (Protozoa, Ciliophora): New hypotheses based on multigene information and identification of localized incongruence. *Public Library of Science ONE, 6*, e17471. doi:10.1371/journal.pone.0017471

Zhao, X., Gao, S., Fan, Y., Strüeder-Kypke, M., & Huang, J. (2015). Phylogenetic framework of the systematically confused *Anteholosticha−Holosticha* complex (Ciliophora, Hypotrichia) based on multigene analysis. *Molecular Phylogenetics and Evolution, 91*, 238−247. doi:10.1016/j.ympev.2015.05.021

Associate Editor: Thorsten Stoeck